Room-temperature Coulomb staircase in semiconducting InP nanowires modulated with light illumination

# Room-temperature Coulomb staircase in semiconducting InP nanowires modulated with light illumination

**Toshishige Yamada**[1,2,5]**, Hidenori Yamada**[3]**, Andrew J Lohn**[2,4] **and Nobuhiko P Kobayashi**[2,4]

[1] Center for Nanostructures, School of Engineering, Santa Clara University, Santa Clara, CA 95053, USA
[2] Department of Electrical Engineering, Baskin School of Engineering, University of California, Santa Cruz, CA 95064, USA
[3] Department of Electrical and Computer Engineering, University of California, San Diego, CA 92092, USA
[4] Nanostructured Energy Conversion Technology and Research (NECTAR), Advanced Studies Laboratories, University of California, Santa Cruz and NASA Ames Research Center, Moffett Field, CA 94035, USA

E-mail: tyamada@scu.edu

## Abstract

Detailed electron transport analysis is performed for an ensemble of conical indium phosphide nanowires bridging two hydrogenated $n^+$-silicon electrodes. The current–voltage ($I$–$V$) characteristics exhibit a Coulomb staircase in the dark with a period of ∼1 V at room temperature. The staircase is found to disappear under light illumination. This observation can be explained by assuming the presence of a tiny Coulomb island, and its existence is possible due to the large surface depletion region created within contributing nanowires. Electrons tunnel in and out of the Coulomb island, resulting in the Coulomb staircase $I$–$V$. Applying light illumination raises the electron quasi-Fermi level and the tunneling barriers are buried, causing the Coulomb staircase to disappear.

(Some figures in this article are in colour only in the electronic version)

## 1. Introduction

Since the careful study of its unintentional doping mechanism [1], indium phosphide (InP) has been attracting a lot of attention, and during the last ten years, InP nanowires (NWs) have been studied extensively in terms of their growth, device fabrication, and characterization [2–15]. The progress in this field is reviewed in [16]. Kobayashi *et al* reported In NW synthesis and electrical transport measurements on a simple photoconductor under light illumination [17]. On their photoconductor with two hydrogenated Si (Si:H) electrodes, InP was grown into cone-shaped nanowires with bases attached on the electrodes as shown in figures 1(a) and (b), where the detail of the growth is the same as that in [17]. Some

of the NWs encountered each other during the growth and fused together in pairs as in figure 1(c), establishing an electrical connection. Since the Si:H electrodes were $n^+$-doped and the InP was unintentionally n-doped regardless of synthesis methods, electrons dominantly contributed to the electrical transport. In this paper, we describe detailed analysis on the DC electron transport characteristics of the InP NW photoconductor in the dark and under light illumination with monochromatic light (633 nm, 1.95 eV) at various optical power levels ranging up to 5 $\mu$W. Multiple batches of photoconductor devices were fabricated and characterized in [17], but the dark characteristics have never been analyzed. The light energy is well beyond the InP direct band gap $E_g$ of 1.34 eV so that appreciable electron–hole (e–h) pair generation is expected. We have compared the responses for a 633 nm light capable of exciting both InP and a-Si:H, and a 780 nm

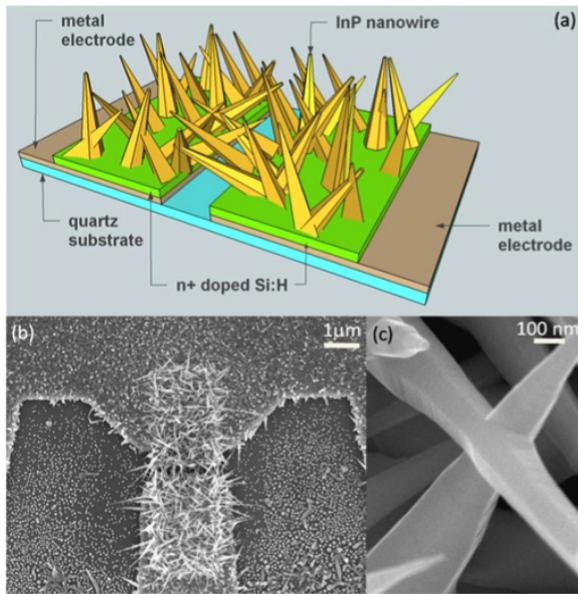[5] Author to whom any correspondence should be addressed.

**Figure 1.** (a) Schematic of a fabricated InP nanowire (NW) photoconductor. (b) Scanning electron microscope (SEM) image (top view) of a representative InP NW photoconductor. InP NWs were selectively grown on the pair of $n^+$-doped Si:H electrodes. (c) SEM image of a point where two nanowires were fused.



**Figure 2.** (a) $I_d$ as a function of $V_d$ with light power as a parameter, 0 $\mu$W in the dark, 0.64 $\mu$W, 1.1 $\mu$W, 2.1 $\mu$W, 2.6 $\mu$W, 3.7 $\mu$W, and 5.0 $\mu$W, respectively. (b) Fourier transform of $I_d(V_d) - cV_d$, where $c$ is a constant. The peak is at $2\pi/V = 6.6$ V$^{-1}$, corresponding to the staircase period of $\Delta V = 0.95$ V.

test light capable of exciting only InP, and confirmed that the conductance increase certainly came from InP, and not from the electrodes. One electrode (drain) was biased at $V_d = -5$–5 V while the other (source) was grounded, and the current $I_d$ flowing into and out of these electrodes was measured. It has to be emphasized that all data were taken at room temperature.

We have examined several devices, and have observed increasing photoconductor conductance as the illumination power is increased due to the e–h generation. Nearly half of the devices showed a smooth $I_d$–$V_d$ curve in the dark with a slight diverging nonlinearity ($d^2 I_d/dV_d^2 > 0$ when $V_d > 0$, or $d^2 I_d/dV_d^2 < 0$ when $V_d < 0$) and the NW differential conductance between the electrodes $R_{NW} = dI_d/V_d$ changed from ~2 nS at $V_d = 0$ to ~5 nS at $V_d = 5$ V. The illumination increased the device photoconductivity by orders of magnitude, which is quite important in the engineering context, but was well understood in the physics context as discussed in [17]. An example of smooth $I_d$–$V_d$ characteristics is discussed in figure 3 of [18]. However, the remaining devices showed an unusual $I_d$–$V_d$ behavior in the dark as detailed below and it gradually disappeared under illumination. The measurement equipment is just a simple prober without any signal processing capabilities. Because the smooth and staircase characteristics co-existed using the same measurement equipment, this is not any artifact of the measurement equipment. The present paper focuses on the behavior of these devices, and we propose its physical origin—a Coulomb staircase. According to our interpretation, this would be one of the first articles reporting a Coulomb staircase modulated optically, by light illumination.

## 2. Staircase current–voltage characteristics

The resulting plot of $I_d$ versus $V_d$ is shown in figure 2(a) with light illumination power indicated in $\mu$W under which
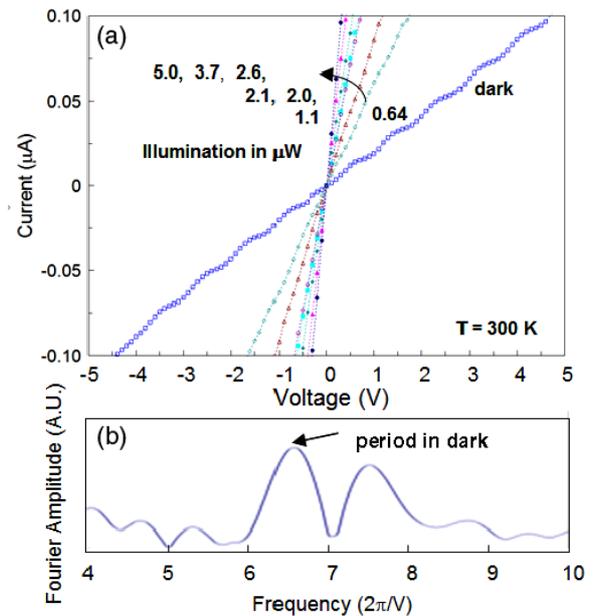
a specific $I_d$–$V_d$ curve is collected. The photoconductor conductance increases approximately 0.06 $\mu$S with each $\mu$W increment of power, and reaches an order of magnitude higher value at 5 $\mu$W. As clearly seen in figure 2(a), there are substantial differences in the $I_d$–$V_d$ curve in the dark compared to those under light illumination. $I_d$ increases discretely with $V_d$, demonstrating evident periodic staircase characteristics in the dark. To extract the staircase period $\Delta V$ in the dark, we have subtracted the linear component of the current, and then performed a Fourier transform as in figure 2(b). The peak is reached at $2\pi/\Delta V = 6.6$ V$^{-1}$ or $\Delta V = 0.95$ V. We have also examined the data by plotting $d^2 I_d/dV_d^2$ and performing Fourier transformation, which led us to practically identical results. Under light illumination at 0.64 $\mu$W, the weak wavy characteristics associated with the periodic staircase still remain with smaller $\Delta V$ while the linear component is noticeably large. However, the NW photoconductor shows Ohmic characteristics under light illumination at 1.1 $\mu$W and higher: $I_d$ increases smoothly as $V_d$ increases and the staircase disappears. These changes are reversible, i.e., the $I_d$–$V_d$ characteristics in the dark are identical even after going through progressive illumination cycles. Devices with the staircase in the dark exhibit $dI_d/dV_d \sim I_d/V_d \sim 10$ nS ($I_d$–$V_d$ is linear if neglecting the staircase fine structure), while those without the staircase exhibit $dI_d/dV_d \sim 2$ nS at $V_d = 0$ and ~5 nS at $V_d = 5$ V.

The $I_d$–$V_d$ characteristics collected in the dark are reminiscent of a Coulomb staircase [19–27], which is typical for a structure of 'conductor–tunneling barrier (capacitor)–Coulomb island–tunneling barrier (capacitor)–conductor' as shown in the inset to figure 3(a). We here use thermodynamics
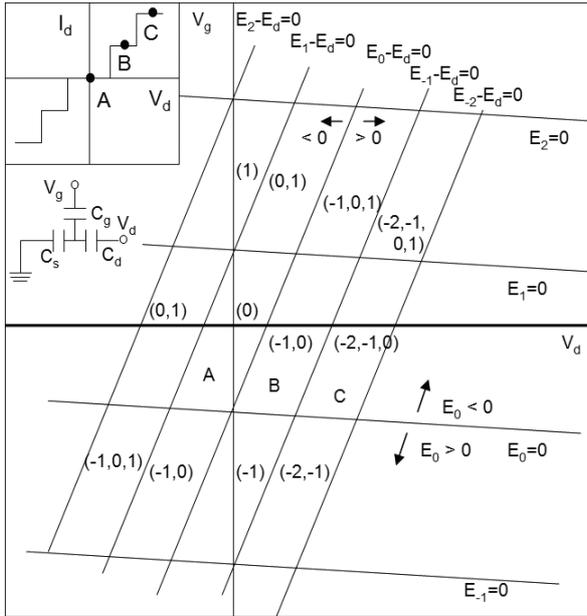
**Figure 3.** Internal energy change $\Delta(N, k) = E_N - E_k$ after incoming electron tunneling to the island from electrode $k$ in the $V_g$–$V_d$ plane. If $E_N - E_k < 0$, an electron tunnels in from electrode $k$ to the island with $N$ final electrons (the island electrons change from $N - 1$ to $N$). If $E_N - E_k > 0$, an electron tunnels out from the island with $N$ initial electrons to electrode $k$ (the island electrons change from $N$ to $N - 1$).

and describe the Coulomb staircase in a more intuitive way [22–27]. Two conditions must be satisfied: (i) the Coulomb charging energy is much larger than the ambient thermal energy $k_B T$; (ii) the tunneling resistance $R_T$ is much larger than the quantum resistance of $R_Q = h/2q^2 = 12.9$ k$\Omega$, with $h$ the Planck constant and $q$ the unit charge. Generally, the minimum internal energy and maximum entropy requirements conflict and thus we usually minimize the free energy $F(N) = U(N) - TS$ at given temperature $T$, where $U(N)$ is the internal energy when the island has $N$ electrons and $S$ is the entropy. However, because of condition (i), the internal energy $U$ is dominant in $F$ (or $F \sim U$) and the minimization of $U$ will explain the essential physics. We consider a capacitance circuit as in the inset of figure 3 with the source capacitor $C_s$ grounded ($V_s = 0$), the drain capacitor $C_d$ biased at $V_d$, and the gate capacitor $C_g$ biased at $V_g$. The gate electrode with a $C_g$ is included for better description of the thermodynamics even though it is absent in our experiment (we can take a limit of $C_g \to 0$ and $V_g \to 0$ with no tunneling possibility from/to the gate electrode). The change $\Delta U$ is evaluated for an incoming electron tunneling event from electrode $k$ ($k = $ s or d) to the island, where the number of electrons changes from $N - 1$ to $N$. Because of condition (ii), electrons are isolated on the island and their numbers are quantized[6]. The island gains the Coulomb energy by $U_C(N) - U_C(N - 1)$, where $U_C(N) = (Nq)^2/2C$ and $C = C_s + C_d + C_g$ is the island capacitance. The potential energy also changes with this tunneling because

---

[6] When the island is not isolated well (high tunneling probability), an electron can co-exist in the electrodes as well as the island. Then, the number of electrons on the island is not quantized.

electrode $k$ loses $-|q|V_k$ and the island gains $-|q|V_{islnd}$, where $V_{islnd} = (C_d V_d + C_g V_g)/C$ is an island voltage. The resultant $\Delta U$ is therefore given by

$$\Delta U(N, k) = U_C(N) - U_C(N - 1) \\ - |q|(C_d V_d + C_g V_g)/C + |q|V_k. \tag{1}$$

By introducing new variables

$$E_N = U_C(N) - U_C(N - 1) - |q|(C_d V_d + C_g V_g)/C, \tag{2}$$

$$E_k = -|q|V_k, \tag{3}$$

we have

$$\Delta U(N, s) = E_N - E_s = E_N, \tag{4}$$

$$\Delta U(N, d) = E_N - E_d. \tag{5}$$

The rules guiding tunneling are as follows.

(i) If $\Delta U(N, k) = E_N - E_k < 0$, an electron tunnels in from electrode $k$ to the island with $N$ final electrons (the island electrons change from $N - 1$ to $N$).

(ii) If $\Delta U(N, k) = E_N - E_k > 0$, an electron tunnels out from the island with $N$ initial electrons to electrode $k$ (the island electrons change from $N$ to $N - 1$).

Figure 3 is a diagram of how $E_N$ and $E_N - E_d$ change in the $V_g$–$V_d$ plane, where the $V_d$ axis ($V_g = 0$) is our interest. Considering our staircase characteristics with a clear period, it is assumed that the pair of tunneling capacitances are asymmetric, i.e., $C_d \ll C_s$. In fact, otherwise, lines for $E_N = 0$ will have an appreciable negative slope and intersect with the $V_d$ axis, resulting in a disturbed staircase period. Depending on $V_d$, there are parallelogram regions corresponding to each step of the staircase, A, B, and C, in figure 3. The signs of $E_N$ and $E_N - E_d$ are listed in figures 4(a)–(c) and the evolution of $N$ is indicated, respectively.

In region A in figure 4(a), when $N \leqslant -1$, $E_N < 0$ and $E_N - E_d < 0$, and this means when the island has $-1$ electrons or less (larger negative numbers), incoming tunneling of an electron from the source or drain occurs until the island has zero electrons. When $N \geqslant 0$, $E_N > 0$ and $E_N - E_d > 0$, and this means when the island has $+1$ electrons or more, outgoing tunneling of an electron to the source or drain occurs until the island has zero electrons. Thus, zero drain current flows in the steady state with $N = 1$.

In region B in figure 4(b), the source shows the same behavior as that in region A. However, the drain shows a different behavior due to increased $V_d > 0$, i.e., when $N \leqslant 0$, $E_N - E_d < 0$, and $N \geqslant 1$, $E_N - E_d > 0$. Thus, the island can take $N = -1$ or 0. Suppose $N = -1$. An electron tunnels in from the source because $E_0 < 0$ while incoming tunneling from the drain is forbidden because $E_0 - E_d > 0$, and then $N = 0$. The same electron tunnels out to the drain because $E_0 - E_d > 0$ while outgoing tunneling to the source is forbidden because $E_0 < 0$, and then $N = -1$. This completes one cycle. In this process, current carried by a single electron flows from the drain to source.

In region C in figure 4(c), the source shows the same behavior as that in regions A and B. However, the drain shows a further different behavior due to further increased $V_d > 0$,
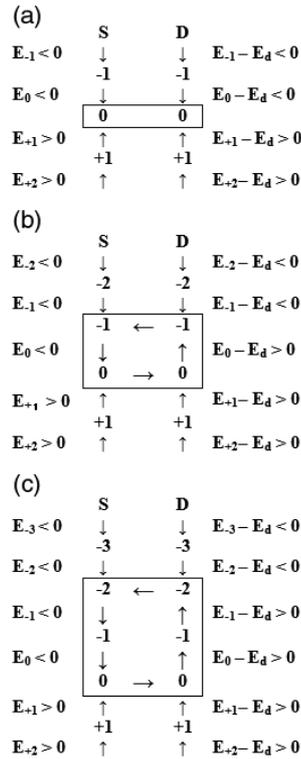
(a)

|  | S | D |  |
|---|---|---|---|
| $E_{-1} < 0$ | ↓ | ↓ | $E_{-1} - E_d < 0$ |
|  | -1 | -1 |  |
| $E_0 < 0$ | ↓ | ↓ | $E_0 - E_d < 0$ |
|  | 0 | 0 |  |
| $E_{+1} > 0$ | ↑ | ↑ | $E_{+1} - E_d > 0$ |
|  | +1 | +1 |  |
| $E_{+2} > 0$ | ↑ | ↑ | $E_{+2} - E_d > 0$ |

(b)

|  | S | D |  |
|---|---|---|---|
| $E_{-2} < 0$ | ↓ | ↓ | $E_{-2} - E_d < 0$ |
|  | -2 | -2 |  |
| $E_{-1} < 0$ | ↓ | ↓ | $E_{-1} - E_d < 0$ |
|  | -1 | ← | -1 |
| $E_0 < 0$ | ↓ | ↑ | $E_0 - E_d > 0$ |
|  | 0 | → | 0 |
| $E_{+1} > 0$ | ↑ | ↑ | $E_{+1} - E_d > 0$ |
|  | +1 | +1 |  |
| $E_{+2} > 0$ | ↑ | ↑ | $E_{+2} - E_d > 0$ |

(c)

|  | S | D |  |
|---|---|---|---|
| $E_{-3} < 0$ | ↓ | ↓ | $E_{-3} - E_d < 0$ |
|  | -3 | -3 |  |
| $E_{-2} < 0$ | ↓ | ↓ | $E_{-2} - E_d < 0$ |
|  | -2 | ← | -2 |
| $E_{-1} < 0$ | ↓ | ↑ | $E_{-1} - E_d > 0$ |
|  | -1 | -1 |  |
| $E_0 < 0$ | ↓ | ↑ | $E_0 - E_d > 0$ |
|  | 0 | → | 0 |
| $E_{+1} > 0$ | ↑ | ↑ | $E_{+1} - E_d > 0$ |
|  | +1 | +1 |  |
| $E_{+2} > 0$ | ↑ | ↑ | $E_{+2} - E_d > 0$ |

**Figure 4.** Evolution in the number of electrons on the island for different biases $V_d$. (a) Region A of zero current, where the number of thermodynamically allowed island electrons ($N$) is 0, (b) region B of unit current with $N = -1$ and 0, and (c) region C of two units of current with $N = -2$, $-1$, and 0. Arrows indicate how tunneling occurs and $N$ changes.

i.e., when $N \leqslant 0$, $E_N - E_d < 0$, and when $N \geqslant 1$, $E_N - E_d > 0$. Thus, the island can take $N = -2, -1$, or 0. Suppose $N = -2$. An electron tunnels in from the source because $E_{-1} < 0$ while outgoing tunneling from the drain is forbidden because $E_{-1} - E_d < 0$, and then $N = -1$. Another electron tunnels in from the source successively because $E_0 < 0$ while outgoing tunneling to the source is forbidden because $E_{-1} - E_d > 0$, and then $N = 0$. Then, one of these two electrons tunnels out to the drain because $E_0 - E_d > 0$ while outgoing tunneling to the source is forbidden because $E_0 < 0$, and then $N = -1$. The remaining electron tunnels out to the drain because $E_{-1} - E_d > 0$ while outgoing tunneling to the source is forbidden because $E_{-1} < 0$, and then $N = -2$. This completes one cycle. The current carried by two electrons flows from the drain to source.

If we assume that it takes almost the same time $\tau$ to complete each cycle, then the drain current is 0 for region A, $|q|/\tau$ for region B, and $2|q|/\tau$ for region C, etc.

Tunneling barriers will act as tunneling capacitors in the equivalent circuit picture. When this structure is embedded in our system of Si:H electrode—fused InP NW—Si:H electrode, the Coulomb staircase will be observed if (i) the Coulomb charging energy is much larger than the ambient thermal energy $k_B T$, and (ii) the tunneling resistance $R_T$ is much larger than the quantum resistance of $R_Q = h/2q^2 = 12.9$ kΩ, so that the island is isolated and can accommodate an integer number of electrons [27] (also see footnote 6). Then, spatially

correlated successive tunneling of an electron from source to drain occurs and the Coulomb staircase results [22–27]. Our analysis below strongly suggests that the Coulomb staircase is exhibited at room temperature.

## 3. Analysis of experiment

We first examine the influence of illumination on the staircase qualitatively. In the dark, the Fermi level $E_{F0}$ is well below the two tunneling barriers corresponding to capacitors $C_s$ and $C_d$. When an electron tunnels to the island, the charging energy is $\sim q^2/C_\Sigma$, where $C_\Sigma = C_s + C_d$. The charging energy is comparable to $q \Delta V = 0.95$ eV and is much larger than $k_B T = 26$ meV. The total resistance $R_{tot}$ reflecting $R_T$ is in the 10 MΩ range, much larger than $R_Q = 12.9$ kΩ. Therefore, the staircase $I_d$–$V_d$ characteristics are seen in the dark [22–27]. Under light illumination, a lot of e–h pairs are generated and $E_{F0}$ splits into quasi-Fermi levels for electrons $E_{Fn}$ and holes $E_{Fp}$. $E_{Fn}$ will rise as the light illumination power $P$ is increased, from $E_{F0}$ to $E_{Fn1}$ in the schematic energy diagram of the inset to figure 5(a). $\Delta V$ decreases at $P = 0.64$ μW compared to that in the dark, and this is consistent with decreasing $1/C_s$ and $1/C_d$ (due to the effective reduction of the capacitor–plate distance) with rising $E_{Fn}$ with $P$. When $E_{Fn}$ rises to $E_{Fn2}$, the tunneling barriers are mostly located below it and these capacitors practically disappear ($1/C_s$ and $1/C_d \to 0$). As a result, the system can be regarded as a simple resistor, and linear $I_d$–$V_d$ characteristics result with a much lower resistance. This scenario is all consistent with our experimental observations. In the following, we will analyze the experimental data quantitatively, and show that this scenario is in fact a conceivable explanation for our unique NW photoconductor behavior in the dark and under light illumination.

The model assumes a single active Coulomb island on a pair of NWs while our structural analysis (figure 1) clearly shows multiple fused NW pairs bridging two electrodes (we have identified twelve NW pairs on average present per photoconductor) [17]. Since these NW pairs are connected to Si:H electrodes in parallel, the assumption is equivalent to one pair having resistance substantially lower than the other pairs, and determines overall $I_d$–$V_d$ characteristics. This is a legitimate assertion since $R_T$ through the above barriers will be an important source of resistance. In fact, tunneling transport is widely seen in various nanoscale systems, and $R_T$ depends on the tunnel barrier width exponentially. As a result, $R_T$ can change by an order of magnitude even with a very small atomic scale change of ~0.1 nm in the tunneling barrier width [28]. Since the microscopic details of the multiple fused NW pairs are all different, there would be appreciable variations in the tunneling barrier among the NW pairs, resulting in significant difference (orders of magnitude) in $R_T$.

To further extend the view, two tunneling barriers are also highly likely to be asymmetric, and the tunneling resistance for one barrier can be an order of magnitude different from that for the other. In this case the barrier with less tunneling dominates transport, and the staircase period $\Delta V$ is $q/C_i$, where $C_i$ is the dominant barrier capacitance ($i = s$ or $d$)
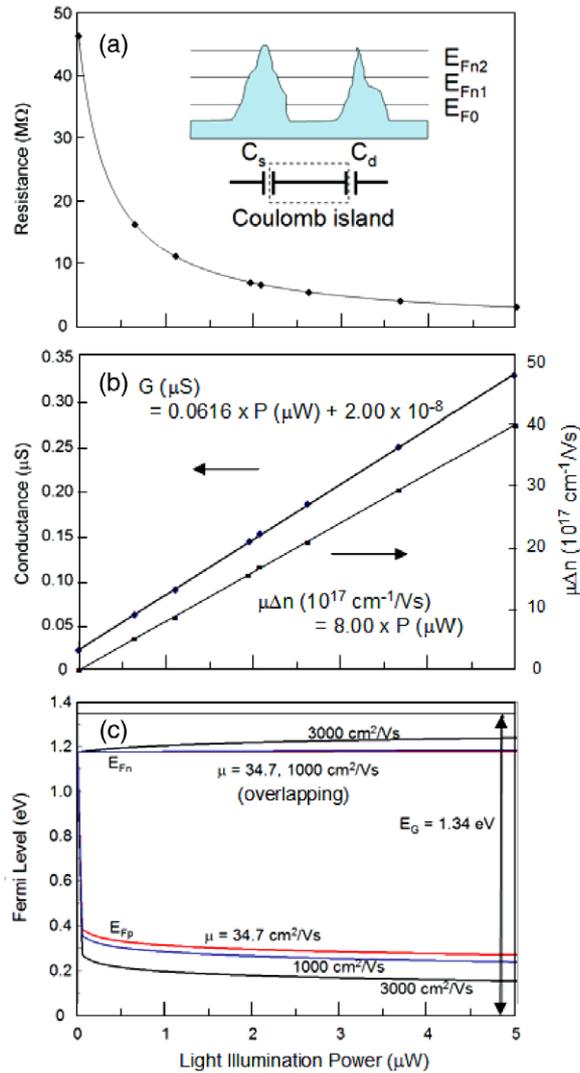
**Figure 5.** (a) Resistance $R_{tot}$ as a function of light illumination power $P$, where each dot represents a measured point. Inset: schematic energy band diagrams for a Coulomb island and barriers for Fermi levels $E_{F0}$, $E_{F1}$, and $E_{F2}$. (b) Conductance $G$ and $\mu \Delta n$ as a function of $P$. (c) $E_{Fn}$ and $E_{Fp}$ as a function of $P$ for representative electron mobility $\mu$ values, 34.7,[7] 1000, and 3000 cm$^2$ V$^{-1}$ s$^{-1}$.

[19]. From figure 2(b), $\Delta V = 0.95$ V and this suggests the presence of very small capacitances in the range of 0.1 aF in a NW pair. $C_i$ can be given by $C_i = \alpha \times \varepsilon A/d$ even when the plate area $A$ and the distance squared $d^2$ are comparable, where $\alpha$ is a dimensionless factor ($\sim 10^0$) representing the capacitance fringing field effects [29]. Using this expression, we estimate that the physical dimension of these capacitors is a rectangular prism of $A = 10$ nm$^2$ and $d \sim 0.5$ nm with a vacuum dielectric constant $\varepsilon \sim 1$ (the tunneling barrier corresponding to a vacuum gap in the InP background). In some devices, the staircase characteristics are not observed, and this is interpreted as the necessary pair of capacitors not being successfully formed, resulting in the staircaseless smooth $I_d$–$V_d$ characteristics.

These capacitors are significantly smaller than the typical NW radius of $\sim 0.1$ $\mu$m around the fused portion. However, the fact that InP NWs are unintentionally doped semiconductors and their surfaces are largely depleted suggests that it is not the physical dimension of the fused portion that accounts for the capacitance. Unintentionally doped InP thin films synthesized by metal-organic chemical vapor deposition are usually n-type with an electron density of $n \sim 10^{15}$ cm$^{-3}$, while unintentionally doped InP thin films grown by molecular beam epitaxy (MBE) from solid sources are consistently n-type with $n \sim 10^{16}$ cm$^{-3}$ (in exceptional cases, $n \sim 5 \times 10^{14}$ to $5 \times 10^{15}$ cm$^{-3}$ is reported in MBE grown InP) [1]. We have confirmed that our unintentionally doped InP blanket films are n-type with $n \sim 10^{15}$ cm$^{-3}$. This means that our significantly wide NWs can have $n \sim 10^{15}$ cm$^{-3}$, but our narrow NWs could have up to $n \sim 10^{16}$ cm$^{-3}$. The depletion region width $w_{dep}$ is estimated with the abrupt planar junction formula $(2\varepsilon V_{surf}/qn)^{1/2}$ using the depletion approximation [30], where $\varepsilon$ is an InP dielectric constant 12.5 with respect to that of vacuum, $V_{surf}$ is a surface potential. Assuming $V_{surf} \sim 0.1$ eV ($V_{surf}$ is a fraction of $E_g$ [31]), we estimate $w_{dep} \sim 0.3$ $\mu$m for $n = 10^{15}$ cm$^{-3}$, and $w_{dep} \sim 0.1$ $\mu$m for $n = 10^{16}$ cm$^{-3}$. The staircase scenario demands that the radius and $w_{dep}$ be comparable near the fused portion of cone-shaped NWs whose radii are $\sim 0.1$ $\mu$m and[8] that there be an active conducting region near the NW central axis. If we consider that there would be a possibility of systematic increased doping (thermodynamic or kinetic), e.g., $n \sim 10^{16}$ cm$^{-3}$ towards the tip of the NWs, everything is consistent with our proposed mechanisms to explain the experimental observations: NW devices are electrically conducting even though NWs are connected via fused portions of $\sim 0.1$ $\mu$m and $\sim 10$ nm$^2 \times$ 0.5 nm rectangular prism capacitors exist near the Coulomb island deep inside the NWs.

Because of large $w_{dep}$, it would be highly possible that capacitances of $\sim 10$ nm$^2 \times$ 0.5 nm rectangular prisms are present within much wider NWs. In fact, this is an important and substantial difference between metallic and semiconducting nanostructures. In metals, $w_{dep} \sim 0$ due to large $n$, and once the capacitor physical size is estimated in modeling, identifying the capacitor location would be straightforward. After capacitor size estimation, Hanna and Tinkham suggested that capacitors should be located between the scanning tunneling microscope (STM) tip and metallic sample, and proved it through their observation of $I_d$–$V_d$ modulation when changing the STM–sample distance [19]. Matsumoto *et al* created a surrounding barrier and a resultant metallic Coulomb island with pre-designed dimension by oxidizing a metallic layer with an STM tip, and confirmed that the staircase period was consistent with the barrier dimension [20]. In these works, $w_{dep} \sim 0$ in metals plays a critical role. However, in semiconducting NWs, $w_{dep}$ is large due to small $n$ and, thus, the active NW region contributing to electron transport is much deeper in location and much

---

[7] The mobility is significantly underestimated and cannot be smaller than this value, since the surface depletion and the barriers causing the Coulomb staircase are not considered.

[8] In the depletion approximation, the charge distribution is approximated with a step function, but the real charge density changes smoothly with location. $w_{dep} \sim$ radius means that there will be some conducting charges available deep inside the NW.

narrower in radius than the actual NW size. Because of large $w_{dep}$, it is conceivable that two small capacitors of $\sim 10$ nm$^2 \times$ 0.5 nm rectangular prisms can exist in NWs, in particular around the fused portion. We consider the island to be located in the fused portion and coupled to the source and drain NWs. Understanding how the source and drain NWs fuse, including the crystal orientation of the fused portion with respect to the NWs, will be important in clarifying the physical origin and properties of the island and its surrounding potential barrier. Our $I_d$–$V_d$ staircase is clear so that it would not be necessary to consider the coupling of multiple capacitors [32, 33].

Since Si:H electrodes are n$^+$-doped and InP NWs are unintentionally n-doped [17], and the bulk electron mobility is several ten times higher than the bulk hole mobility, we assume that only electrons contribute to transport. Given the characteristics of the two-probe measurement, $R_{tot}$ reflects two different contributions, contact resistance $R_c$ between the electrodes and NWs, and NW bulk resistance $R_{NW}$. Thus, $R_{tot} = R_c + R_{NW}$. In figure 5(a), $R_{tot}$ is plotted as a function of light illumination power $P$. In figure 5(b), $G(P) = 1/R_{tot}(P)$ and $\Delta G(P) = G(P) - G(0)$ are plotted. We assume $R_{NW} \gg R_c$. For a cone NW, $R_{NW}$ is given by

$$\int_0^h \rho \, dz/[\pi r^2(z)] = \rho h/(\pi r_t r_b), \qquad (6)$$

where $\rho$ is the InP resistivity and $r(z)$ is the radius at height $z$ with $r(h) = r_t$ and $r(0) = r_b$. Then, $\Delta G$ is expressed as $qA/L \times \mu \Delta n$ with the electron mobility $\mu$, the e–h pair density $\Delta n$, the length $L$, and the effective cross-section $A = \pi r_t r_b$ of the NW. Without the knowledge of $\mu$ in our NWs, $\mu \Delta n$ is plotted as a function of $P$. Both $G(P)$ and $\Delta G(P)$ show apparent linearity. This is consistent with our starting assumption of $R_{NW} \gg R_c$. In fact, although $R_{NW} \propto 1/P$, $R_c$ generally depends on $P$ differently. If $R_{NW} \sim R_c$, the apparent linearity of $G(P)$ cannot be observed. The linearity suggests that $R_{NW} \gg R_c$, $R_{tot} \sim R_{NW}$, and $Dn \propto P$.

Now $R_{NW} = R_{bulk} + R_T$, where $R_{bulk}$ represents the NW bulk resistance. $R_{bulk}$ varies little while $R_T$ changes significantly (because of exponential barrier width dependence) among different fused NW pairs. The linearity of $G(P)$ further suggests that $R_{bulk} \gg R_T$. Also, the Coulomb staircase requires isolation of the island, i.e., $R_T \gg R_Q$ [27]. Thus, in the dark when the clear staircase is observable, $R_{bulk} \sim 10$ M$\Omega \gg R_T \gg R_Q = 12.9$ k$\Omega$ for the fused NW pair dominating the photoconductor's characteristics. For the other non-dominant fused NW pairs, $R_T > $ (or $\gg$) $R_{bulk} \sim$ 10 M$\Omega$ and the resultant $R_{tot}$ is much higher so that practically no current flows in these parallel connections. Under light illumination when the staircase disappears, $R_T \leqslant R_Q = $ 12.9 k$\Omega$ and $R_{tot} \sim R_{bulk}$ is reinforced for the dominant NW pair. In some photoconductors, the staircase was absent even in the dark, and this is interpreted as $C_s$ and $C_d$ not small enough or $R_T \gg R_Q = 12.9$ k$\Omega$ not satisfied.

Next, we will discuss how $E_{F0}$ in the dark is modulated by $P$ in InP. When $n \sim 10^{14}$–$10^{15}$ cm$^{-3}$, $E_{F0}$ is located at 1.115– 1.175 eV above the top of the valence band $E_v$ ($E_g = 1.34$ eV). Using e–h effective masses of 0.08 and 0.623, the effective conduction-band and valence-band densities $N_c$ and $N_v$ are

$5.7 \times 10^{17}$ cm$^{-3}$ and $1.1 \times 10^{19}$ cm$^{-3}$, respectively. Thus, the intrinsic carrier density $n_i$ is $\sqrt{N_c N_v} e^{-Eg/2k_B T} = 10^7$ cm$^{-3}$. $P$ creates the same density of excess e–h pairs $\Delta n = \Delta p$. In figure 5(c),

$$E_{Fn} = k_B T \ln[1 + (\Delta n + n_0)/n_i] + E_{F0}, \qquad (7a)$$

$$E_{Fp} = -k_B T \ln(1 + \Delta p/n_i) + E_{F0} \qquad (7b)$$

are plotted as a function of $P$. There is no practical difference in $E_{Fn}$ between $n_0 = 10^{14}$ and $10^{15}$ cm$^{-3}$ except for $P = 0$. The electron mobility $\mu$ was not measured and was unknown. $E_{Fn}$ and $E_{Fp}$ were calculated for representative values, $\mu = $ 34.7 cm$^2$ V$^{-1}$ s$^{-1}$ (a theoretical lower limit for a cone-shaped NW with $n \sim 10^{15}$ cm$^{-3}$ (see footnote 8)), 1000 cm$^2$ V$^{-1}$ s$^{-1}$, and 3000 cm$^2$ V$^{-1}$ s$^{-1}$ (an upper limit for intrinsic bulk InP). When $P = 1$ $\mu$W, however, the quasi-Fermi levels are fairly insensitive to $\mu$, and $E_{Fn} \sim 1.2$ eV and $E_{Fp} \sim 0.30$ eV. With further increase in $P$, $E_{Fn}$ increases and $E_{Fp}$ decreases gradually. For $P = 0$–5 $\mu$W, $\Delta E_{Fn} = 25$–85 meV. When the potential barriers are comparable to $\Delta E_{Fn}$, the Coulomb staircase scenario should appear. The $I_d$–$V_d$ curve in the dark has a finite slope near $V_d = 0$ and this indicates that there was an initial 'effective' charge on the Coulomb island [19], and this gives information on the physical origin of the barriers, which we have not identified at this stage.

In [3], a Coulomb oscillation was discussed: the behavior of $I_d$ as a function of gate voltage $V_g$ at fixed drain $V_d$, caused by unintentionally created small Coulomb islands on the InP NW. The $V_g$ period was about 1 mV.

In [4], a Coulomb staircase was discussed: the behavior of $I_d$ as a function of $V_d$ at fixed $V_g$. A similar disappearance of the Coulomb staircase to our case was observed, by increasing backgate voltage $V_g$ for an InAs NW with a pair of barriers created with 100 nm separated InP segments. An InAs NW provided a conducting route for electrons, and InP segments created a pair of potential barriers. In their experiment, a Coulomb staircase was observed with the $V_d$ period of about 5 mV at $V_g = 23$ mV, and this is interpreted in our model as the electron Fermi level still being below the potential barriers, just like our $E_{Fn1}$ in figure 5(a). However, when $V_g$ was increased to 31 mV, the Coulomb staircase almost disappeared. According to our model, more electrons were attracted in the InAs NW with larger $V_g$ and the electron Fermi level was raised. As a result, the electron Fermi level was mostly above the potential barriers, just like our $E_{Fn2}$ in figure 5(a). In their experiment, they raised the electron Fermi level electronically (by applying larger $V_g$) and observed the disappearance of the Coulomb staircase. In our case, we have raised the electron quasi-Fermi level optically (by applying light illumination) and observed the disappearance of the Coulomb staircase. Our model can provide a simple explanation for both experiments based on the relation between the electron Fermi level and the potential barriers.

## 4. Conclusion

We have analyzed DC $I_d$–$V_d$ characteristics of InP NWs between two n$^+$-Si:H electrodes in the dark and under light

illumination. The $I_d$–$V_d$ curve in the dark exhibits periodic staircase steps. When the NWs are illuminated, the staircase features are suppressed and the $I_d$–$V_d$ curve is Ohmic. The change is reversible by returning to the dark. We have shown that everything can be explained consistently with the optically modulated Coulomb staircase scenario.

(i) InP NWs are unintentionally doped at $n \sim 10^{15}$ cm$^{-3}$ when the radius is significantly large, but near the NW fusion when the radius is 0.1 $\mu$m, $w_{dep}$ is expected to be of the order of or less than $\sim$0.1 $\mu$m with $n \sim 10^{16}$ cm$^{-3}$ to be consistent with the experimental observation that all devices show electrical conduction. Because of this large $w_{dep}$, an active conducting region is deep inside the NW, near the central axis.

(ii) Two tunneling barriers surround a Coulomb island around the fused portion of NWs, where the NW radius and $w_{dep}$ are comparable. The barriers are considered as two series capacitors of $\sim$0.1 aF and are estimated as $\sim$10 nm$^2 \times$ 0.5 nm rectangular prisms in size, which are much smaller than the fused portion due to large $w_{dep}$. Devices without the staircase do not have these pairs of capacitors and simply show the usual staircaseless $I_d$–$V_d$ characteristics.

(iii) Although there are multiple NW pairs connecting two electrodes, only one pair determines the entire electrical characteristics because $R_T$ depends exponentially on the barrier width, and $R_{tot}$ of a fused NW pair varies significantly from one to another.

(iv) In the dark, $E_{F0}$ is located at $\sim$1.2 eV above $E_v$. Under light illumination with power up to 5 $\mu$W, $E_{Fn}$ rises by $\Delta E_{Fn} = 25$–85 meV. The effective barrier height should be comparable to this $\Delta E_{Fn}$.

## Acknowledgments

## References

[1] Martin T, Stanley C R, Iliadis A, Whitehouse C R and Sykes D R 1985 *Appl. Phys. Lett.* **46** 994
[2] Duan X, Huang Y, Cui Y, Wang J and Lieber C M 2001 *Nature* **409** 66
[3] De Franceschi S, van Dam J A, Bakkers E P A M, Feiner L F, Gurevich L and Kouwenhoven L P 2003 *Appl. Phys. Lett.* **83** 344
[4] Thelander C, Martensson T, Bjork M T, Ohlsson B J, Larsson M W, Wallenberg L R and Samuelson L 2003 *Appl. Phys. Lett.* **83** 2052
[5] Krishnamachari U, Borgstrom M, Ohlsson B J, Panev N, Samuelson L, Seifert W, Larsson M W and Wallenberg L R 2004 *Appl. Phys. Lett.* **85** 2077
[6] Mohan P, Motohisa J and Fukui T 2005 *Nanotechnology* **16** 2903
[7] Mattila M, Hakkarainen T, Mulot M and Lipsanen H 2006 *Nanotechnology* **17** 1580
[8] Ding Y, Motohisa J, Hua B, Hara H and Fukui T 2007 *Nano Lett.* **7** 3598
[9] Bao J, Bell D C, Capasso F, Wagner J B, Mårtensson T, Trägårdh J and Samuelson L 2008 *Nano Lett.* **8** 836
[10] Chuang L C, Moewe M, Crankshaw S and Chang-Hasnain C 2008 *Appl. Phys. Lett.* **92** 013121
[11] Novotny C J, Yu E T and Yu P K L 2008 *Nano Lett.* **8** 775
[12] van Weert M H M, Akopian N, Perinetti U, van Kouwen M P, Algra R E, Verheijen M A, Bakkers E P A M, Kouwenhoven L P and Zwiller V 2009 *Nano Lett.* **9** 1989
[13] Caroff P, Dick K A, Johansson J, Messing M E, Deppert K and Samuelson L 2009 *Nat. Nanotechnol.* **4** 50
[14] Pemasiri K *et al* 2009 *Nano Lett.* **9** 648
[15] Poole P J, Lefebvre J and Fraser J 2009 *Appl. Phys. Lett.* **83** 2055
[16] Yan R, Gargas D and Yang P 2009 *Nat. Photon.* **3** 569
[17] Kobayashi N P, Logeeswaran V J, Islam M S, Li X, Straznicky J, Wang S Y, Williams R S and Chen Y 2007 *Appl. Phys. Lett.* **91** 113116
[18] Sarkar A, Logeeswaran V J, Kobayashi N P, Straznicky J, Wang S Y, Williams R S and Islam M S 2007 *Proc. SPIE* **6768** 67680P
[19] Hanna A E and Tinkham M 1991 *Phys. Rev.* B **44** 5919
[20] Matsumoto K, Ishii M, Segawa K, Oka Y, Vartanian B J and Harris J S 1996 *Appl. Phys. Lett.* **68** 34
[21] Andres R P, Bein T, Dorogi M, Feng S, Henderson J I, Kubiak C P, Mahoney W, Osifchin R G and Reifenberger R 1996 *Science* **272** 1323
[22] Averin D A and Likharev K K 1991 *Mesoscopic Phenomena in Solids* ed B A Altshuler, P A Lee and R A Webb (Amsterdam: Elsevier) chapter 6
[23] Grabert H and Devoret M H (ed) 1992 *Single Charge Tunneling: Coulomb Blockade Phenomena in Nanostructures* (New York: Plenum)
[24] Tamura H, Hasuo S and Okabe Y 1987 *J. Appl. Phys.* **62** 3036
[25] Beenakker C W J 1991 *Phys. Rev.* B **44** 1646
[26] Amman M, Wilkins R, Ben-Jacob E, Maker P D and Jaklevic R C 1991 *Phys. Rev.* B **43** 1146
[27] Yamada T 2004 *Carbon Nanotubes: Science and Applications* ed M Meyyappan (Boca Raton, FL: CRC Press) chapter 7 (Nanoelectronics Applications)
[28] Yamada T 2001 *Appl. Phys. Lett.* **78** 1739
[29] Sloggett G J, Barton N G and Spenser S J 1986 *J. Phys. A: Math. Gen.* **19** 2725
[30] Shockley W 1976 *Electrons and Holes in Semiconductors, with Applications to Transistor electronics* (Malabar, FL: Krieger)
[31] Bardeen J 1947 *Phys. Rev.* **71** 717
[32] Bar-Sadeh E, Goldstein Y, Zhang C, Deng H, Abeles B and Millo O 1994 *Phys. Rev.* B **50** 8961
[33] Imamura H, Chiba J, Mitani S, Takanashi K, Takahashi S, Maekawa S and Fujimori H 2000 *Phys. Rev.* B **61** 46